

# Stability of strongly anisotropic thin epitaxial film in a wetting interaction with elastic substrate

M. Khenner<sup>1</sup>

<sup>1</sup>*Department of Mathematics, Western Kentucky University, Bowling Green, KY 42101*

(Dated: February 4, 2019)

## Abstract

The linear dispersion relation for longwave surface perturbations, as derived by Levine *et al.* *Phys. Rev. B* **75**, 205312 (2007) is extended to include a smooth surface energy anisotropy function with a variable anisotropy strength (from weak to strong, such that sharp corners and slightly curved facets occur on the corresponding Wulff shape). Through detailed parametric studies it is shown that a combination of a wetting interaction and strong anisotropy, and even a wetting interaction alone results in complicated linear stability characteristics of strained and unstrained films.

PACS numbers: 68.55.-a

## I. INTRODUCTION

Studies of the morphological instabilities of a thin solid films are a first step towards understanding complex phenomena such as the formation of a three-dimensional nanoscale islands in strained alloy heteroepitaxy. Such studies became common after the pioneering works of Asaro and Tiller [1], Grinfeld [2] and Srolovitz [3]. The classical Asaro-Tiller-Grinfeld instability is one of an uniaxially stressed solid film on a rigid infinite substrate. Its variants for the single-component and alloy films on the rigid as well as on the deformable substrates have been studied and this research continues. Reviews of works on the single-component films have been published, see for instance Ref. [4].

Film-substrate wetting interaction is a relatively new concept in the field of research on morphological instability and evolution [5–7]. Since such interaction provides one possible mechanism capable of terminating unlimited pattern coarsening [8, 9, 11], the focus in the majority of modeling papers published to-date is, quite understandably, on the analysis of weakly nonlinear instability that gives rise to the formation of a pattern of structures, or on the direct numerical simulation of a fully nonlinear problem.

In Ref. [8] it is recognized that in the presence of wetting interaction characterized by an additional wetting energy that depends on the local film thickness  $h$ , the boundary conditions that describe stress balance at the film free surface and at the film-substrate interface must be augmented by *wetting stress* terms that are proportional to the rate of change of the surface energy with  $h$ . As a consequence of solution of the elastic free-boundary problem with such boundary conditions, the contributions from wetting potential and misfit strain are coupled in the expression for the growth rate of small perturbations (through the term proportional to the misfit parameter), and they also enter separately in other terms in the growth rate. Some stability characteristics have been analyzed in Ref. [8], but the surface energy is assumed isotropic (which leaves only one source of instability - the epitaxial stress) and the parameter space is not fully explored. This paper attempts to fill this gap. We show that very nontrivial linear stability emerges when the film thickness is less than roughly ten times the characteristic wetting length.

We remark here that at least one model has been published where wetting stress is not accounted for and thus contributions from wetting potential and strain are decoupled in the dispersion relation [10, 11]. Due to such decoupling the resulting stability characteristics are

much simpler than those revealed in Ref. [8] and in this paper, despite that the substrate is taken deformable and the solution of the elasticity problem is more complicated.

## II. PROBLEM STATEMENT

Following Refs. [8, 12], we consider a dislocation-free, one-dimensional, single-crystal, epitaxially strained thin solid film in a wetting interaction with a solid, semi-infinite elastic substrate. The film surface  $z = h(x, t)$  evolves due to surface diffusion. This evolution is described by

$$\frac{\partial h}{\partial t} = \frac{\Omega DN}{kT} \frac{\partial}{\partial x} \left[ \left( 1 + \left( \frac{\partial h}{\partial x} \right)^2 \right)^{-1/2} \frac{\partial \mathcal{M}}{\partial x} \right], \quad (1)$$

where  $\Omega$  is the atomic volume,  $D$  is the adatoms diffusivity,  $N$  is the adatoms surface density,  $kT$  is the Boltzmann factor, and  $\mathcal{M}$  is the surface chemical potential. The latter has contributions from the elastic energy in the film, the anisotropic surface energy, and a wetting interaction:

$$\begin{aligned} \mathcal{M} = \mathcal{E}(h) + \Omega \left[ \left( \gamma + \frac{\partial^2 \gamma}{\partial \theta^2} \right) \kappa - \delta \left( \frac{\kappa^3}{2} + \frac{\partial^2 \kappa}{\partial S^2} \right) \right] + \\ \Omega \left( 1 + \left( \frac{\partial h}{\partial x} \right)^2 \right)^{-1/2} \frac{\partial \gamma}{\partial h}, \end{aligned} \quad (2)$$

where  $\gamma(h, \theta)$  is the height- and orientation-dependent surface energy,  $\kappa$  is the curvature of the surface, and  $S$  is the arclength along the surface. The term proportional to the small positive parameter  $\delta$  is the regularization that is required in view of ill-posedness of Eq. (1) for strong anisotropy ( $\epsilon_\gamma > 1/15$  in Eq. (4) below) [13–16]. The two-layer exponential model for the surface energy reads [5, 7]:

$$\gamma(h, \theta) = \gamma_t(\theta) + (\gamma_s - \gamma_t(\theta)) \exp(-h/\ell), \quad (3)$$

where  $\gamma_s$  is the surface energy of the substrate when there is no film,  $\theta$  is the angle that the unit surface normal makes with the reference direction (chosen along the  $z$ -axis),  $\ell$  is characteristic wetting length, and  $\gamma_t(\theta)$  is the four-fold anisotropic surface energy of a thick film:

$$\gamma_t(\theta) = \gamma_0(1 + \epsilon_\gamma \cos 4\theta), \quad \epsilon_\gamma \geq 0. \quad (4)$$

Here  $\gamma_0$  is the mean surface energy and  $\epsilon_\gamma$  is the strength of anisotropy. This model has been shown the most accurate to-date [17, 18].

The expression for the elastic energy  $\mathcal{E}(h)$  in Eq. (2) is derived in Ref. [12] in the longwave approximation and without accounting for wetting interaction. Wetting interaction is included into the longwave framework in several papers, including Refs. [8, 10] In Ref. [8] the surface energy  $\gamma_t$  is assumed isotropic ( $\epsilon_\gamma = 0$ , thus  $\gamma_t = \gamma_0$ ), and therefore the two-layer exponential form is

$$\gamma(h) = \gamma_0 + (\gamma_s - \gamma_0) \exp(-h/\ell). \quad (5)$$

Correspondingly,  $\delta$  is taken zero in the chemical potential, since regularization is not needed when anisotropy is zero or is weak. On the other hand, in Ref. [19] the dispersion relation is derived in the longwave limit for the unstrained film in a wetting interaction with the substrate through the strongly anisotropic surface energy given in Eqs. (3) and (4). Thus by simply combining the expressions from Refs. [8] and [19] we can proceed to the linear stability analysis of the strained anisotropic film with wetting interaction. To this end, we choose  $\ell$  as the length scale,  $\ell^2/D$  as the time scale and state the dimensionless linear growth rate:

$$\begin{aligned} \omega(h_0, k, \mu, \epsilon, \epsilon_\gamma) = & A\epsilon^2 (\mu + A_1 h_0 k) k^3 - \\ & B\epsilon [\mu (h_0 - 1) + h_0 (B_1 h_0 - B_2) k] k^3 a \exp(-h_0) + \\ & F [(\Lambda - (G + \Lambda) \exp(-h_0)) k^4 - \Delta k^6 - a \exp(-h_0) k^2]. \end{aligned} \quad (6)$$

Here  $k$  is the wavenumber of the perturbation,  $\epsilon$  is the misfit strain in the film,  $\mu = \mu_f/\mu_s$  is the ratio of the film shear modulus to the substrate shear modulus, and  $h_0$  is the uniform thickness of unperturbed planar film. Other parameters are:

$$A = \frac{8N\Omega^2\alpha_s(1+\nu_f)^2\mu_s}{kT\ell\alpha_f^2}, \quad B = \frac{4N\Omega^2\gamma_0\alpha_s(1+\nu_f)\nu_f}{kT\ell^2\alpha_f^2}, \quad (7)$$

$$A_1 = \frac{2(C_1 - \alpha_f)}{\alpha_f\alpha_s}, \quad B_1 = \frac{C_2}{2\alpha_f\alpha_s\nu_f}, \quad B_2 = \frac{2C_1}{\alpha_f\alpha_s}, \quad (8)$$

$$C_1 = \alpha_f + \alpha_f\beta_s\mu - \alpha_s^2\mu^2, \quad C_2 = 4\alpha_f + 3\alpha_f\beta_s\mu - 4\alpha_s^2\mu^2, \quad (9)$$

$$\alpha_{f(s)} = 2(1 - \nu_{f(s)}), \quad \beta_{f(s)} = 1 - 2\nu_{f(s)}, \quad (10)$$

$$F = \frac{N\Omega^2\gamma_0}{kT\ell^2}, \quad \Delta = \frac{\delta}{\gamma_0\ell^2}, \quad (11)$$

$$\Lambda = 15\epsilon_\gamma - 1, \quad G = \gamma_s/\gamma_0, \quad a = G - 1 - \epsilon_\gamma. \quad (12)$$

In Eqs. (7)-(10)  $\nu$  is Poisson's ratio. Note coupling of wetting and strain through the term proportional to  $\epsilon$  in the second line of Eq. (6). This term would not be present were wetting

stress is omitted from the formulation of the elasticity problem in Ref. [8]; the only terms due to wetting potential that are present in that case are in the third line of the equation [10, 19].

Our goal is to characterize film stability in the space of dimensionless parameters  $h_0$ ,  $k$ ,  $\mu$ ,  $\epsilon$  and  $\epsilon_\gamma$ . Other material parameters will be fixed to their most characteristic values. We choose the following values:  $D = 1.5 \times 10^{-6}$  cm<sup>2</sup>/s,  $N = 10^{15}$  cm<sup>-2</sup>,  $\Omega = 2 \times 10^{-23}$  cm<sup>3</sup>,  $kT = 1.12 \times 10^{-13}$  erg,  $\gamma_0 = 2 \times 10^3$  erg/cm<sup>2</sup>,  $\gamma_s = 2\gamma_0$ ,  $\nu_f = 0.198$ ,  $\nu_s = 0.217$ ,  $\mu_f = 10^{12}$  erg/cm<sup>3</sup>,  $\delta = 5 \times 10^{-12}$  erg, and  $\ell = 3 \times 10^{-8}$  cm. The value of the characteristic wetting length is of the order of 1 ML thickness for InAs or Ge film [17]. Unless noted otherwise, we assume strong anisotropy, i.e.  $\epsilon_\gamma > 1/15$  and thus  $\Lambda > 0$ . However, we assume  $a > 0$ , which imposes the limitation  $\epsilon_\gamma < G - 1$ . With  $G = 2$  (value corresponding to the chosen  $\gamma_0$  and  $\gamma_s$ ), this gives  $\epsilon_\gamma < 1$ .

### III. UNSTRAINED FILM

For the case of zero misfit strain it is easy to obtain the concise criteria of film stability (from Eq. (6)). It follows that the perturbations with the wavenumbers larger than  $k_c = \sqrt{\Lambda/\Delta}$  cannot destabilize a film of any thickness (that is,  $\omega < 0$  for  $k > k_c$  and any  $h_0$ ). However, in the opposite case  $k < k_c$  only the films of thickness that is less than the critical,  $h_0^{(c_1)}$ , are stable:

$$h_0 < h_0^{(c_1)} = -\ln \frac{\Lambda k^2 - \Delta k^4}{a + (G + \Lambda)k^2}. \quad (13)$$

With  $\Delta = 25/9$  corresponding to the material parameters stated above, and  $\epsilon_\gamma = 0.1$ , we obtain  $k_c = 0.42$ . Taking typical  $k = 0.1k_c$  in Eq. (13) gives  $h_0^{(c_1)} = 6.94$ , which translates to the dimensional value of 7 ML. Stronger anisotropy decreases  $h_0^{(c_1)}$ . We notice also that strong anisotropy destabilizes (that is, the contribution proportional to  $k^4$  in the square bracket is positive) only relatively thick films, such that

$$h_0 > h_0^{(c_2)} = -\ln \frac{\Lambda}{G + \Lambda}. \quad (14)$$

For the chosen values,  $h_0^{(c_2)} = 1.6$  ML. Such threshold-type influence of strong anisotropy is distinctly different from the simplified model in which wetting interaction is not accounted for. The latter model can be obtained by taking  $h_0 \rightarrow \infty$  in Eq. (6), and thus this equation becomes  $\omega(k, \epsilon_\gamma) = F(\Lambda k^4 - \Delta k^6)$ , from which it is clear that strong anisotropy has destabilizing influence on a film of arbitrary thickness. These findings to some extent echo

Refs. [17, 20], where the existence of the critical perturbation amplitude that is necessary to destabilize a film in the presence of a cusp in the surface energy  $\gamma(\theta)$  (which is the case below the roughening temperature), has been demonstrated. Thus if a film is thin, critical amplitude may be unattainable and the film will not be destabilized. However, it must be noted that the analysis in Refs. [17, 20] includes stress from the outset, and therefore it is difficult to separate the effects of stress and energy there.

Finally, we make the following remark concerning *non-wetting* films ( $a < 0$ ). One example of such material system may be the energetically-driven dewetting of silicon-on-insulator [21]. Repeating the analysis and referring to the critical values shown above, it follows that film of any thickness is stable with respect to perturbations with wavenumbers larger than  $\max(k_c, k_c^{(u)})$ , where  $k_c^{(u)} = \sqrt{-a/(G + \Lambda)}$ . If  $k_c < k < k_c^{(u)}$ , then film is stable if  $h_0 > h_0^{(c1)}$  and unstable otherwise. If  $k_c^{(u)} < k < k_c$ , then the film is stable if  $h_0 < h_0^{(c1)}$  and unstable otherwise. Finally, if  $k < \min(k_c, k_c^{(u)})$ , then the film of any thickness is unstable. With  $G = 0.5$  and  $\epsilon_\gamma = 0.1$ ,  $k_c^{(u)} = 0.77 > k_c$ , and therefore the third possibility,  $k_c^{(u)} < k < k_c$ , must be dismissed. Typically, the second scenario ( $k_c < k < k_c^{(u)}$ ) holds, and thus there is a critical thickness below which the film is unstable [9]. We will not further consider non-wetting films in this paper.

#### IV. STRAINED FILM

Since the growth rate  $\omega$  is quadratic in  $\epsilon$ , one can determine the boundaries of neutral stability,  $\omega = 0$ , in the  $h_0 - \epsilon$  plane. This has been done in Ref. [8] for the case of isotropic surface energy. It will be demonstrated below that even without anisotropy the stability is more complicated than follows from the analysis presented in Ref. [8]. Our primary objective is to investigate how the strong surface energy anisotropy influences stability. It must be emphasized that in the presence of wetting interaction the expression for the growth rate, Eq. (6), contains the term that is proportional to the first power of misfit strain. But whether this term is destabilizing or stabilizing (for  $a > 0$ ) depends on the sign of the product  $\epsilon [\mu(h_0 - 1) + h_0(B_1 h_0 - B_2)k]$ . Typically, only for sufficiently small  $\mu$  ( $\mu < 1.13$  for  $h_0 = 2, k = 0.1$  and values of other parameters as cited in Sec. II) this product is positive (negative) when  $\epsilon > 0 (< 0)$ , and then the second term in Eq. (6) is stabilizing. Some implications of the broken symmetry between the tensile and the compressive strain that are manifested by the second term in Eq. (6) can be seen in Fig. 4.

### A. Isotropic surface energy ( $\epsilon_\gamma = \Delta = 0$ )

For several values of  $\mu$  Fig. 1(a-d) shows the zero-level contour of the discriminant,  $d(h_0, k)$ , of the quadratic equation for  $\epsilon$ . Two types of domains are present, ones where  $d > 0$  and others where  $d < 0$ . In a domain  $d < 0$ , the surface can't be neutrally stable and thus it has to be either stable or unstable in the entire domain for *all* values of  $\epsilon$ . Thus the sign of the growth rate at one randomly chosen point in a domain  $d < 0$  determines whether surface is absolutely stable or unstable there. [23]

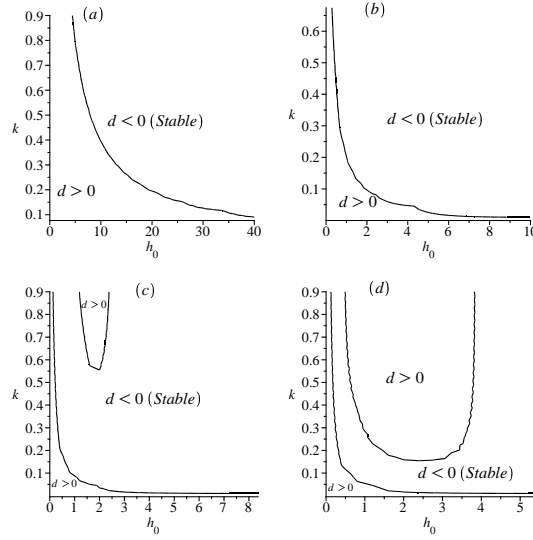


FIG. 1: Domains of negative ( $d < 0$ ) and positive ( $d > 0$ ) discriminant of the quadratic equation  $\omega = 0$  for  $\epsilon$ , where  $\omega$  is given by Eq. (6).  $\epsilon_\gamma = 0$ . (a)-(d):  $\mu = 0.5, 3, 6.5, 10$ . Domains of “absolute” stability or instability are marked by “Stable” or “Unstable”.

For  $\mu < 0.5$ ,  $d > 0$  in the entire plane, and the typical neutral curves for this situation are shown in Fig. 2. Notice that here stability becomes absolute when the film is sufficiently thick. Referring to Fig. 1(a-d), the neutral stability curves for  $k = 0.1$  and  $\mu = 0.5, 3, 6.5, 10$  are shown in Fig. 3. As  $\mu$  increases an absolute stability emerges for smaller film thickness. This critical thickness corresponds to the intersection of the horizontal line  $k = 0.1$  with the boundary of the domain  $d < 0$ . For  $\mu = 6.5$  and 10 there is also another domain where  $d > 0$  (situated at larger, but still small values of  $k$  where the longwave approximation is valid). As  $\mu$  increases this domain becomes larger and at  $\mu = 50$  the gap between two zero

level curves closes. The neutral stability curves for  $\mu = 10$  and  $k = 0.2, 0.4$  (inside the upper  $d > 0$  domain in Fig. 1(d)) are shown in Fig. 4. In this case it is obvious that only a tensile strain ( $\epsilon > 0$ ) can result in instability. Thick films are stable, as well as thin, weakly strained films.

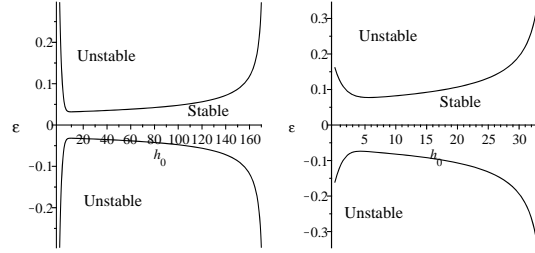


FIG. 2: Neutral stability curves for  $\mu = 0.4$ ,  $\epsilon_\gamma = 0$ , and (a):  $k = 0.1$ , (b):  $k = 0.5$ .

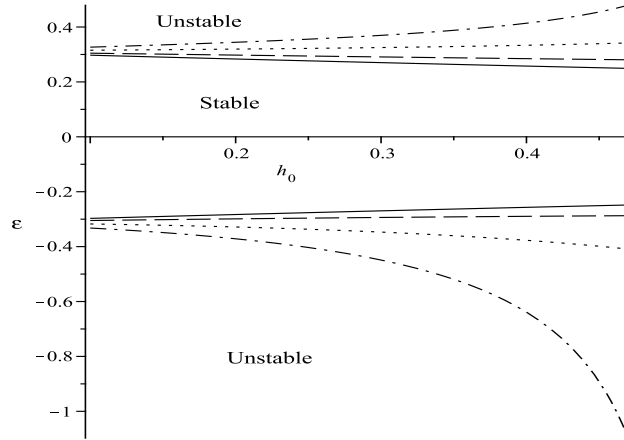


FIG. 3: Neutral stability curves for  $\epsilon_\gamma = 0$ ,  $k = 0.1$ . Solid curve:  $\mu = 0.5$ , dashed curve:  $\mu = 3$ , dot curve:  $\mu = 6.5$ , dash-dotted curve:  $\mu = 10$ . For each value of  $\mu$ , the surface is stable in the domain bounded by two curves of the same style.

Since typical  $\mu$  is around 0.8, the stability diagram for zero anisotropy is of the type shown in Figs. 2 and 3. Similar diagrams were plotted by Levine *et al.* [8]

## B. Strongly anisotropic surface energy

For moderate values of  $\mu$ , we studied the cases  $\epsilon_\gamma = 0.1$  and  $\epsilon_\gamma = 0.9$ .



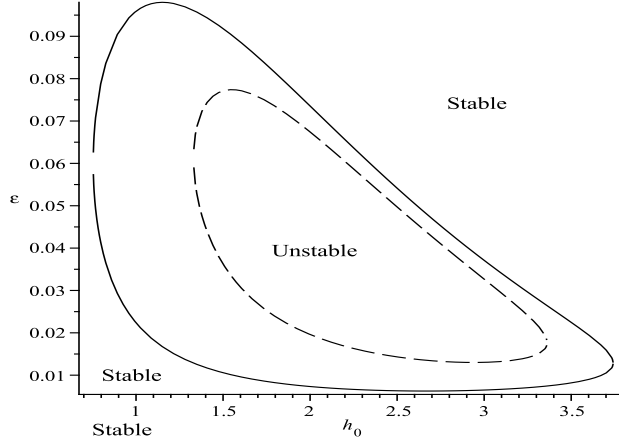


FIG. 4: Neutral stability curves for  $\mu = 10$ ,  $\epsilon_\gamma = 0$ . Solid curve:  $k = 0.4$ , dashed curve:  $k = 0.2$ .

Fig. 5 shows the domains of positive and negative discriminant for  $\mu = 0.4, 0.7, 3$ . For  $\epsilon_\gamma = 0.1$  and  $\mu = 0.4$  there is only one domain  $d > 0$  (where for fixed  $k$  the film can transition from stable to unstable when  $\epsilon$  and  $h_0$  change), while for the other two values of  $\mu$  there is two such domains. For small values of  $h_0$  the only (primary)  $d > 0$  domain in Fig. 5(a) (Fig. 5(b)) includes all relevant wavenumbers. As the anisotropy increases, this domain becomes smaller as it shifts to smaller values of  $h_0$ , but it still includes all relevant wavenumbers. Correspondingly, the domain of absolute instability enlarges in Fig. 5(a) to include almost all wavenumbers and thicknesses. In Fig. 5(b) a large region of absolute instability emerges between two dashed curves. To the right of the rightmost dashed curve, where discriminant is positive for  $\epsilon_\gamma = 0.9$ , stability depends on values of  $\epsilon$  and  $h_0$  for given  $k$ .

For  $\epsilon_\gamma = 0.1$  only, Fig. 6 shows the boundaries of neutral stability for  $\mu = 0.4, 0.7, 3$  and  $k = 0.1$ . The surface is stable in the domains bounded by the curves of the same style, except for the narrow (in  $\epsilon$ ) domain bounded by the dash-dotted curves that start around  $h_0 = 6$ ; in this domain the surface is unstable and thus the domain is marked by the letter “U”. (Naturally, beyond the domains of stability the surface is unstable.) The vertical diamond-style lines mark the “entry” and “exit” points to the  $d < 0$  domain in Fig. 5(c), where the surface is absolutely stable. (In Fig. 5(c) these points are also marked by diamonds.) Notice that unlike the isotropic case shown in Fig. 4, here a quite moderate difference in elastic modulus,  $\mu = 3$ , is sufficient to result in the counter-intuitive response: a thick film is stable (unstable) for large (small) misfit strain. This becomes even more apparent for smaller  $\mu$  and larger wavenumbers, see Fig. 7.

Also for  $\epsilon_\gamma = 0.1$ , Fig. 7 shows the neutral stability curves for  $\mu = 0.7$  and  $k = 0.3$ . Again the vertical diamond-style lines mark the “entry” and “exit” points to the  $d < 0$  domain in Fig. 5(b), where the surface is absolutely unstable. Notice from Figs. 6 and 7 how the bell-shaped stability domains terminate at finite film thickness. We thus conclude that at strong anisotropy, and typically for very long-wavelength perturbations and  $0.4 < \mu < 1$ , only small strain, or only small film thickness are not sufficient for stability - both the strain and the thickness must be small for a film to be stable. This is in stark contrast to the isotropic case, where small enough strain is sufficient to make stable a film of arbitrary thickness (see Figs. 2 and 3).

Next, for  $\mu = 0.8$  and  $\epsilon = 0.01$  Fig. 8 shows the zero level curves of  $\omega(h_0, k)$  for  $\epsilon_\gamma = 0.1, 0.2, 0.9$ . Clearly, at given anisotropy only the sufficiently thick films become unstable. This resonates with the conclusion reached for the unstressed films. As anisotropy increases the film thickness has to decrease in order the film to remain stable. At the same time the interval of unstable wavenumbers becomes larger. (For  $\epsilon_\gamma = 0.1$ : disregarding the small difference in  $\mu$ , the “cut” by the horizontal line  $k = 0.1$  in Fig. 8 corresponds to the “cut” by the horizontal line  $\epsilon = 0.01$  in Fig. 6, meaning that the intersection of the line  $k = 0.1$  with the solid curve in Fig. 8 gives roughly the same value of the critical film thickness as gives the intersection of the line  $\epsilon = 0.01$  with the dashed curve in Fig. 6. For the case  $k = 0.3$  a similar comparison can be made of Figs. 7 and 8.)

Next, we take  $\mu = 0.7$  and  $\epsilon_\gamma = 0.1$  and investigate the effects of changing the energy regularization parameter  $\delta$ . We find that increasing  $\delta$  to  $5 \times 10^{-11}$  erg results in elimination of the smallest  $d > 0$  domain in Fig. 5(b) at the expense of enlarging the upper  $d < 0$  domain and shrinking the lower  $d < 0$  domain. Thus increasing  $\delta$  has an overall stabilizing effect, as expected. Moreover, the unstable region lying to the right of the vertical diamond line and confined between the two curves in Fig. 7 is no longer present. Increasing  $\delta$  even more to  $5 \times 10^{-10}$  erg eliminates the lower  $d < 0$  domain as well, and leaves out only two large domains,  $d > 0$  and  $d < 0$  in Fig. 5(b). Note that regularization energy has been linked to the interaction of atomically high steps on a crystal surface in the corner region between two facets [22], but to our knowledge no measurement or calculation of this energy has been published.

Finally, Fig. 9 shows, as functions of  $\epsilon$ , the usual cut-off wavenumber  $k_c$ , the wavenumber at the maximum  $k_{max}$  and the maximum growth rate  $\omega_{max} = \omega(k_{max})$ , while  $h_0$ ,  $\mu$  and  $\epsilon_\gamma$

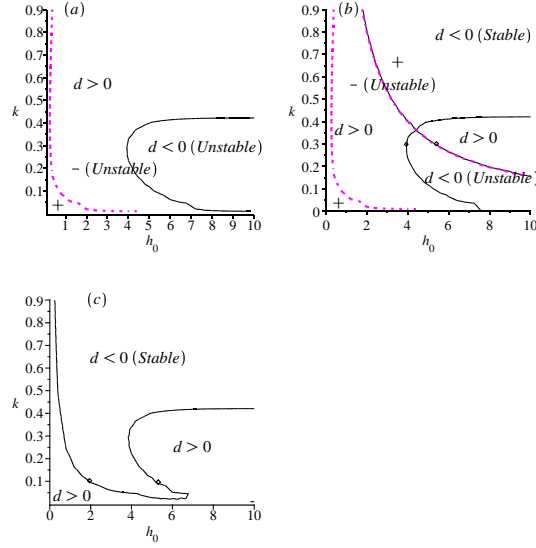


FIG. 5: (Color online.) Domains of negative and positive discriminant of the quadratic equation  $\omega = 0$  for  $\epsilon$ . Solid (dashed) curves correspond to  $\epsilon_\gamma = 0.1$  ( $\epsilon_\gamma = 0.9$ ). Domains of negative and positive discriminant for  $\epsilon_\gamma = 0.1$  case are marked by  $d < 0$  and  $d > 0$ , respectively. Domains of negative and positive discriminant for  $\epsilon_\gamma = 0.9$  case are marked by  $-$  and  $+$ , respectively. (a)-(c):  $\mu = 0.4, 0.7, 3$ .

are held fixed. For  $\epsilon < 0.05871$ ,  $\omega(k) < 0$  for all  $k$ ; for larger values of  $\epsilon$ ,  $\omega > 0$  in some finite interval  $k_0 < k < k_c$  (for example, see the solid curve in the inset of Fig. 8). All three quantities increase with  $\epsilon$ :  $k_c \rightarrow 0.39$ ,  $k_{max} \rightarrow 0.297$ ,  $\omega_{max} \rightarrow 5.428$  as  $\epsilon \rightarrow 1$ , and  $k_0$  decreases until it becomes zero at  $\epsilon = 0.3$ . Thus for  $\epsilon > 0.3$  the growth rate is positive for  $0 < k < k_c$  and negative for  $k > k_c$ .

## V. DISCUSSION AND CONCLUSIONS

It is easy to see that the simultaneous inclusion in Eq. (6) of the stress terms proportional to the first and to the second power of the misfit strain  $\epsilon$  is warranted even when the strain is small. In fact, for the parameter values cited in Section II and for  $\epsilon = 0.01, \mu = 0.8$  (typical values for SiGe and InAs/GaAs films) and longwave perturbations ( $k < 1$ ), the quadratic term is as much as eight times larger than the linear term for small to moderate film thickness ( $h_0 < 10$ ), and it is the only of the two terms remaining in thick films ( $h_0 \rightarrow \infty$ ) where wetting interaction does not influence surface stability and dynamics [12].

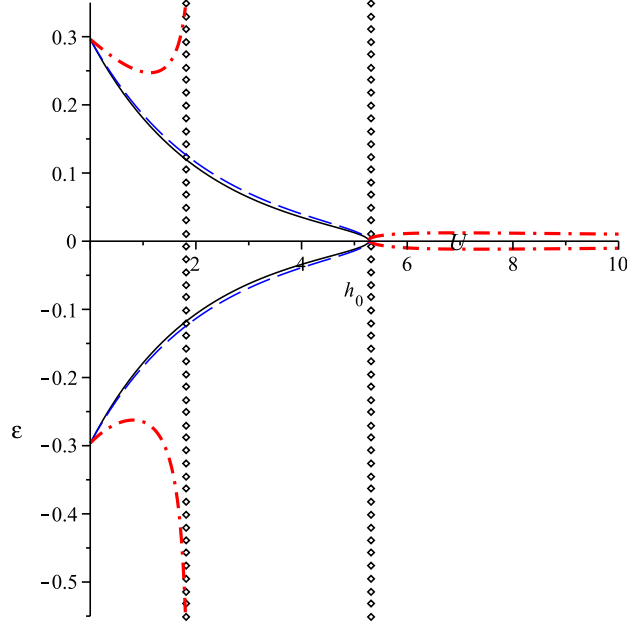


FIG. 6: (Color online.) Neutral stability curves for  $\epsilon_\gamma = 0.1$ ,  $k = 0.1$ . Solid curve:  $\mu = 0.4$ , dashed curve:  $\mu = 0.7$ , dash-dotted curve:  $\mu = 3$ . See text for discussion.

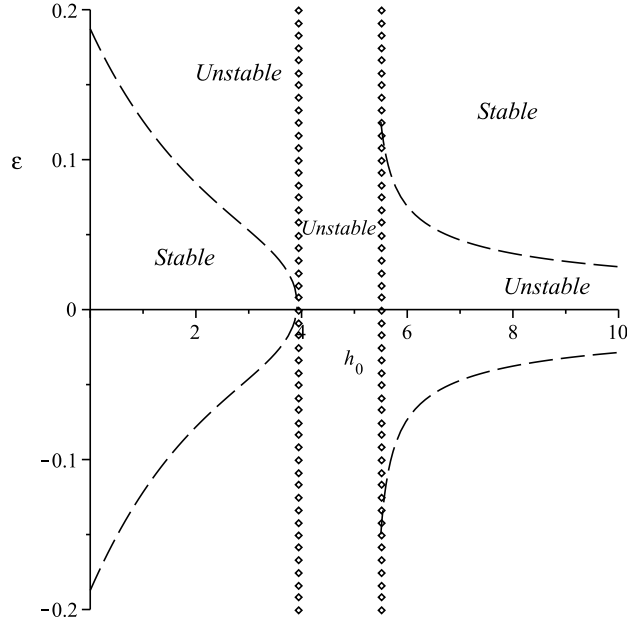


FIG. 7: Neutral stability curves.  $\epsilon_\gamma = 0.1$ ,  $\mu = 0.7$ ,  $k = 0.3$ .

Notice that if anisotropy is zero, then in Eq. (6) the coefficient of  $k^4$  in the square bracket becomes  $-1 - (G - 1) \exp(-h_0)$ , which is simply the negative dimensionless form of  $\gamma(h)$  in

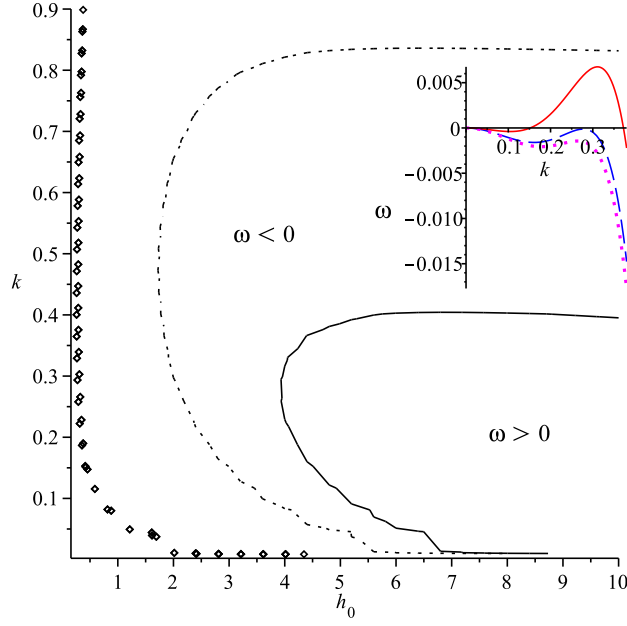


FIG. 8: (Color online.) Curves of  $\omega = 0$  for  $\epsilon_\gamma = 0.1$  (solid),  $\epsilon_\gamma = 0.2$  (dot), and  $\epsilon_\gamma = 0.9$  (diamond).  $\epsilon = 0.01, \mu = 0.8$ . Domains of stability ( $\omega < 0$ ) and instability ( $\omega > 0$ ) are marked for the case  $\epsilon_\gamma = 0.1$ . Inset: dispersion curves  $\omega(k)$  which are obtained when the solid curve is intersected by the vertical lines  $h_0 = 3.8$  (dot curve),  $h_0 = 3.9$  (dashed curve), and  $h_0 = 4.5$  (solid curve).

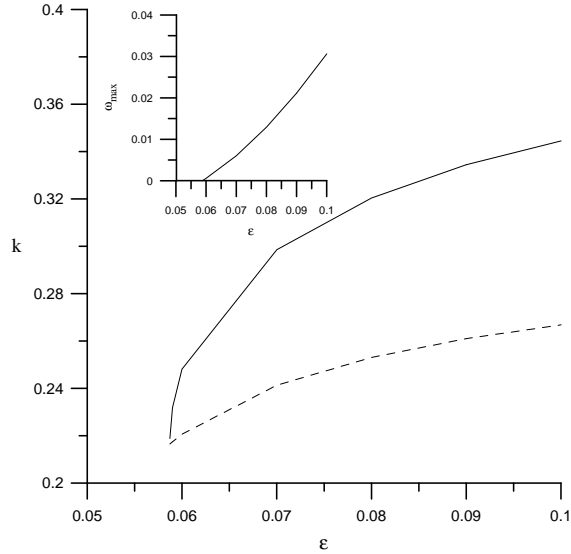


FIG. 9: Solid curve: cut-off wavenumber  $k_c$ ; dashed curve: wavenumber at the maximum of the dispersion curve,  $k_{max}$ , vs.  $\epsilon$ . Inset:  $\omega_{max}$  vs.  $\epsilon$ .  $h_0 = 3, \mu = 0.8$  and  $\epsilon_\gamma = 0.1$ .

Eq. (5). The coefficient of  $k^2$  is the negative dimensionless second derivative of  $\gamma(h)$ .

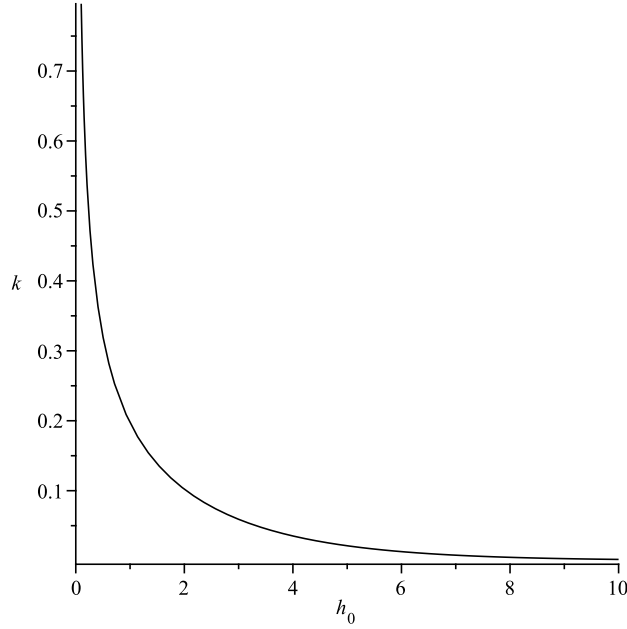


FIG. 10: See text for discussion.

Nonzero anisotropy provides additional terms in  $\omega$ . Up to a positive multiplier  $\epsilon_\gamma$  these terms are  $B\epsilon[\mu(h_0 - 1) + h_0(B_1h_0 - B_2)k]k^3\exp(-h_0)$ ,  $15F(1 - \exp(-h_0))k^4$  and  $F\exp(-h_0)k^2$ . The second and the third terms are positive and therefore destabilizing. For the parameter values used in the paper and  $h_0 = 2, k = 0.1, \epsilon = 0.01$ : the first term is negative for  $\mu > 1.15$  and the sum of all three terms is negative for  $\mu > 31$ . Thus very large  $\mu$  is needed for stabilization of the surface by anisotropy.

The interplay of the film thickness and the perturbation wavenumber in the second and the third terms calls for some additional analysis - notice that the second (third) term increases (decreases) with  $h_0$ . Equating these two terms gives  $k(h_0) = [\exp(-h_0)/15(1 - \exp(-h_0))]^{1/2}$ , which is plotted in Fig. 10. Above (below) the curve the second (third) term dominates. In the limit  $h_0 \rightarrow \infty$  corresponding to the model without wetting interaction (or equivalently to a thick film), the only anisotropic contribution in Eq. (6) that remains is from the second term; it is obviously equal to  $15\epsilon_\gamma Fk^4$ .

To summarize, for an elastic system film/substrate with a wetting interaction through the exponential two-layer wetting model with surface energy anisotropy we considered in detail the linear perturbation growth rate derived in longwave approximation. The growth rate is the complicated function of material parameters, misfit strain, film height, anisotropy

strength and perturbation wavenumber. We chose material parameters that closely mimic SiGe system and plotted stability diagrams, from which we observed a number of novel and, we believe, important features, such as: strong anisotropy destabilizes only relatively thick films (with or without stress); in the case of zero (and, perhaps, weak) anisotropy and large ratio of the film-to-substrate shear modulus  $\mu$  only a tensile strain destabilizes and only films in a fairly narrow range of thickness; in a strongly anisotropic case thick, weakly strained films may be unstable; and, anisotropy (weak or strong) may be overall stabilizing when  $\mu$  is fairly large.

## ACKNOWLEDGMENTS

M.K. acknowledges the support of WKU Faculty Scholarship Council via grants 10-7016 and 10-7054.

- 
- [1] R.J. Asaro and W.A. Tiller, *Metall. Trans.* **3**, 1789 (1972).
  - [2] M.A. Grinfeld, *Sov. Phys. Dokl.* **31**, 831 (1987).
  - [3] D.J. Srolovitz, *Acta Metall.* **37**, 621 (1989).
  - [4] H. Gao and W.D. Nix, *Annu. Rev. Mater. Sci.* **29**, 173 (1999); V.A. Shchukin and D. Bimberg, *Rev. Mod. Phys.* **71**, 1125 (1999).
  - [5] C.-H. Chiu and H. Gao, in: S.P. Baker *et al.* (Eds.), Thin Films: Stresses and Mechanical Properties V, MRS Symposia Proceedings, vol. 356, Materials Research Society, Pittsburgh, 1995, p. 33.
  - [6] Z. Suo and Z. Zhang, *Phys. Rev. B* **58**, 5116 (1998).
  - [7] M. Ortiz, E.A. Repetto, and H. Si, *J. Mech. Phys. Solids* **47**, 697 (1999).
  - [8] M.S. Levine, A.A. Golovin, S.H. Davis, and P.W. Voorhees, *Phys. Rev. B* **75**, 205312 (2007).
  - [9] Y. Pang and R. Huang, *Phys. Rev. B* **74**, 075413 (2006).
  - [10] W.T. Tekalign and B.J. Spencer, *J. Appl. Phys.* **96**, 5505 (2004).
  - [11] M.D. Korzec and P.L. Evans, *Physica D* **239**, 465 (2010).
  - [12] B.J. Spencer, P.W. Voorhees, and S.H. Davis, *J. Appl. Phys.* **73**, 4955 (1993).
  - [13] C. Herring, *Phys. Rev.* **82**, 87 (1951).
  - [14] S. Angenent and M.E. Gurtin, *Arch. Rational Mech. Anal.* **108**, 323 (1989).

- [15] A. Di Carlo, M.E. Gurtin, and P. Podio-Guidugli, *SIAM J. Appl. Math.* **52**, 1111 (1992).
- [16] B.J. Spencer, *Phys. Rev. E* **69**, 011603 (2004).
- [17] S.P.A. Gill and T. Wang, *Surf. Sci.* **602**, 3560 (2008).
- [18] M.J. Beck, A. van de Walle, and M. Asta, *Phys. Rev. B* **70**, 205337 (2004).
- [19] M. Khenner, *Phys. Rev. B* **77**, 165414 (2008); *Math. Model. Nat. Phenom.* **3**, 16 (2008).
- [20] H.R. Eisenberg and D. Kandel, *Phys. Rev. Lett.* **85**, 1286 (2000); *Phys. Rev. B* **66**, 155429 (2002).
- [21] P. Sutter, W. Ernst, Y.S. Choi, and E. Sutter, *Appl. Phys. Lett.* **88**, 141924 (2006).
- [22] A.A. Golovin, S.H. Davis, and A.A. Nepomnyashchy, *Physica D* **122**, 202 (1998).
- [23] Here and below the use of the term “absolute” stability (“absolute” instability) depends on the context. Typically, we use it in a situation when, having *at least two parameters fixed*, and varying other parameters the surface remains stable (unstable). Note also that the formal boundary of longwave region is given by  $k(h_0) = 2\pi/h_0$ , and most characteristic features of the graphs in Fig. 1(a-d) lie below this curve, i.e. in the longwave region.